Case Studies in Construction Materials 16 (2022) e00800

Contents lists available at ScienceDirect

Case Studies in Construction Materials

journal homepage: www.elsevier.com/locate/cscm

Strength and durability properties of geopolymer paver blocks made with fly ash and brick kiln rice husk ash

Shaik Numan Mahdi [a,*], Dushyanth V Babu R [b], Nabil Hossiney [c,*], Mohd Mustafa Al Bakri Abdullah [d]

[a] School of Civil Engineering, CERSSE, JAIN (Deemed to be University), Bangalore, Karnataka, India
[b] School of Civil Engineering, FET-JAIN (Deemed to be University), Bangalore, Karnataka, India
[c] Department of Civil Engineering, CHRIST (Deemed to be University), Bangalore, Karnataka, India
[d] Center of Excellence Geopolymer & Green Technology (CEGeoGTech), Universiti Malaysia Perlis (UniMAP), P.O. Box 77, D/A Pejabat Pos Besar 01000, Kangar, Perlis, Malaysia

ARTICLE INFO

Keywords:
Strength
Durability
Rice husk ash
Geopolymer
Pavers

ABSTRACT

In India the generation of agro waste rice husk ash is abundant. The utilization of rice husk ash in development of geopolymer binders can be suitable to alleviate the environmental problems associated with disposal of rice husk ash. Further, the utilization of rice husk ash generated from the stacks of brick kilns has not been addressed in past, particularly in development of geopolymer binders. This study proposes development of geopolymer paver (GEOPAV) blocks utilizing brick kiln rice husk ash (BKRHA). It presents fresh, mechanical and durability properties of GEOPAV blocks blended with fly ash, BKRHA, natural aggregates, NaOH and Na_2SiO_3 solution, and cured in both sundry and room temperature conditions. Microstructural analysis using scanning electron microscope (SEM) and X-ray diffraction (XRD) was adopted to study the influence of BKRHA on hardened properties of GEOPAV blocks. The results show that addition of BKRHA reduce the workability of GEOPAV mixes due to micro porous surface with honeycombed structure of BKRHA particles. The addition of BKRHA showed negligible improvement in compressive strength of GEOPAV blocks. However, the major advantage was observed with improved split tensile strength and flexural strength for GEOPAV blocks with BKRHA. Further, the durability properties in terms of resistance to acid and frost attack was significantly improved with the addition of BKRHA in GEOPAV blocks. Such improvements can be attributed to high amounts of amorphous silica in BKRHA which contribute towards dissolution and formation of polymeric gel, and thereby serve as a binder to enhance the geopolymer matrix making it dense. Finally, all the developed GEOPAV blocks satisfy the IS 15658–2021 specification requirements and perform much better when compared to commercially available paver blocks.

1. Introduction

Sustainable construction with waste utilization leads to carbon negative environment, which can also be referred to as green environment. For India, the concept of green environment is momentous to mitigate the greenhouse effect originating from various construction practices and generation of industrial waste. Also, to improve the mobility in urban and semi-urban areas, the

* Corresponding authors.
E-mail addresses: shaik.mahdi@gmail.com (S.N. Mahdi), nabil.jalall@christuniversity.in (N. Hossiney).

https://doi.org/10.1016/j.cscm.2021.e00800
Received 31 August 2021; Received in revised form 9 November 2021; Accepted 19 November 2021
Available online 23 November 2021

comprehensive mobility plan has raised the demand on energy intensive construction materials such as Portland cement and filler materials [1]. Therefore, a need arises for alternative cementitious materials in construction industry. Geopolymer technology a type of alkali-activated cementitious material has great potential to incorporate variety type of industrial waste rich in solid aluminosilicates [2–4]. It has shown excellent mechanical and durability properties when used as concrete material [5], and can be one of the preferable binders which can substitute Portland cement in the construction industry [6–8]. Thus, achieving the goal of green environment in the construction industry.

Agro-waste are one of the major sources of pollution in the world today. The utilization of such waste into recycled value-added applications is becoming an important topic to overcome the current environmental situation in the world [9]. A detailed description on the types, classification and use of agro-waste in construction industry can be found in studies published in the past [10,11]. India is the second largest country next to China for milled rice production and has produced approximately 119 million metric tons of milled rice in 2020 [12]. The process of milling gives rice as a staple food product for human consumption by extracting rice husk which accounts to approximately 24 million metric tons. Rice husk, an agro waste by product obtained from the paddy farming is frequently used as a fuel in sustainable technology. Husks of rice are used as a fuel in boilers to produce electricity through the steam generation process [13,14], as well as in kilns of brick industry to stabilize clay bricks by undergoing through a self-burning process [15]. India is world's second-largest manufacturer of burnt clay bricks which accounts for over 10% of global output. It is reported that there are more than 100,000 brick kilns that exist in India, and produce between 150 and 200 billion bricks every year [16]. When agro waste rice husk is used as fuel in between the stacks of industrial brick kilns for burning process, it generates substantial amount of waste rice husk ash (RHA). Agro waste rice husk usage as fuel is identified as one of the green energy practices, but there is a need to deal with the environmental issues associated with RHA. Further, due to lack of proper treatment, RHA is being disposed into landfills or water bodies, which contaminate the environment [17–19]. Thus, the use of rice husk as a fuel cannot be totally termed as "green", if RHA obtained from various industries is not effectively used. Previous attempts have discussed the utilisation of RHA produced from different industrial sources. The black residual RHA, an output of rice mill steam boilers has been used in Portland cement mortar and concrete [20,21]. Rice husk bark ash composed of 65% rice husk with 35% eucalyptus bark collected from a biomass power plant has been utilised for conventional concrete [22], and waste RHA initiated from electric power plants has been used as a partial cement replacement for self-compacting concrete [23]. Also, Pre-processed RHA has shown promise as supplementary binding material in cement concrete [24], self-compacting concrete [25–27], geopolymer concrete [28,29] and concrete blocks [30]. However, pre-processing is time consuming and energy intensive, which reduces its practical applications. Therefore, use of waste RHA without pre-processing will contribute towards economical and sustainable waste management practice. Further, RHA used in the previous studies contains silica in crystalline form which is less reactive. While the agro waste RHA from fired brick kilns contains a high silica content (i.e., about 90%) in amorphous form due to prolonged burning in the brick kilns [31], which is an essential ingredient for the production of geopolymer concrete [32]. Therefore, research to utilize unprocessed brick kiln rice husk ash (BKRHA) in production of geopolymer concrete for various civil engineering applications would be ideal to achieve sustainability in construction.

Paver blocks are unreinforced solid blocks which are pertinent for outdoor applications and are into construction practice for many decades. However, due to growing demand in developing countries and with increasing carbon emissions associated with conventional paver bocks, the need to integrate alternative cementitious or filler materials is becoming one of the current research trends. Some latest studies show the potential of utilizing recycled materials in concrete paver blocks. For instance, replacement of fine aggregate with crushed brick aggregates [33], recycled asphalt aggregates [34,35], recycled crushed glass aggregates and bottom ash aggregates [36] and sludge of drinking water treatment [37] have been investigated. However, based on literature survey there are limited studies pertaining to the use of rice husk ash in geopolymer paver (GEOPAV) blocks. In particular, there are no existing studies on use of BKRHA in GEOPAV blocks. Therefore, the proposed research of utilizing BKRHA in GEOPAV blocks will provide benefits of using excess agro waste and address some of the issues mentioned in aforementioned paragraphs. Further, it will focus on development of paver blocks by integrating alternative cementitious materials, which will reduce the burden on conventional cementitious materials, and thus contribute towards sustainable practice in construction industry.

2. Materials and methods

2.1. Research plan

The activity of this experimental study is as follows; (i) physical and chemical characterization of raw materials, (ii) preparation of geopolymer paver blocks (GEOPAV) synthesized with siliceous pulverized flyash (SPFA), unprocessed BKRHA, natural aggregates and alkaline activators, (iii) curing of GEOPAV subjected to sundried and room temperature conditions, (iv) assessment of strength and durability properties of GEOPAV according to various standards and specifications.

2.2. Materials

The production of GEOPAV includes SPFA, BKRHA, crushed stone aggregates and 12.5 mm down size coarse aggregates. Commercial grade NaOH pellets with 99% purity and water glass (Na_2SiO_3) with a concentration of 18.78% Na_2O, 34.21% SiO_2 and 47% H_2O making a weight ratio of SiO_2 to Na_2O as 1.82 was used as alkali activator. Fly ash was procured from a thermal power station located in Raichur, Karnataka, India, while rice husk ash was obtained from a local brick kiln, which utilizes paddy rice husk as fuel in brick kilns. The collected BKRHA was sieved through 90 μm to select the particles that are compatible with the size of flyash particles, and was considered as supplementary binder in GEOPAV mixture. Fig. 1 shows precursor materials SPFA and BKRHA. Virgin

aggregates were obtained from a local quarry of silk city Ramnagaram, Karnataka, India. Distilled water processed by double distillation plant was used to make the molar concentrations of sodium hydroxide.

2.3. Design synthesis

The geopolymer concrete mixtures were proportioned in order to investigate the potential of using BKRHA in GEOPAV blocks. Further, the percent replacement of BKRHA was based on existing literatures [38,39]. Based on laboratory trials, the various parameters of the GEOPAV mixes were finalized. The density of geopolymer concrete was considered as 2400 kg/m^3 and the total aggregate content was fixed at 71% of the entire mix. The mixes were designed to achieve a target slump of 150 ± 10 mm, with alkaline liquid to binder ratio of 0.56 to achieve good workability for GEOPAV mixes. Table 1 presents the details of mix specifications for GEOPAV blocks. Further, commercial paver blocks made with OPC grade 53 was procured from the local market and considered as control mix, which is denoted as CCP100. The details of the mix proportion for control and GEOPAV blocks is presented in Table 2.

2.4. Production of GEOPAV

GEOPAV specimens were produced in rubber moulds with internal dimensions of 250 mm × 120 mm x 80 mm. Total of 148 specimens were made to evaluate the strength and durability properties of GEOPAV blocks. The 10 M and 12 M solution of NaOH was prepared 24 h prior to the production mix by dissolving NaOH pellets in double distilled water. The alkaline solution was prepared by mixing sodium hydroxide and sodium silicate solution 1 h prior to GEOPAV mixing. Saturated surface dry coarse aggregates (<12.5 mm) and fine aggregates (i.e., crushed stone aggregates, CSD) were prepared for the mix. The aggregates and binders were dry mixed thoroughly in pan mixer for about 2 min. After dry mixing, alkaline solution was added to the pan mixer and mixing continued till the formation of homogenous mix. Workability test was performed using slump cone apparatus and fresh mix was filled in rubber moulds and vibrated simultaneously on 3HP vibrating table. The fresh density was determined before the specimens were subjected to sundried temperature curing (45 ± 2 ℃) for two days, followed by air curing at ambient temperature till the period of 28 days. The strength and durability parameters were evaluated after the assigned curing age on replica of three specimens for each of the different mix types.

2.5. Test methods

The properties of binding materials were confirmed in accordance with ASTM C618, ASTM C114, ASTM C311 and IS 4032. The tests were performed on crushed stone dust and 12.5 mm down aggregates using ASTM C33, ASTM C136/C136M-14 and IS 2386. The precursor materials of GEOPAV were also characterised by various techniques such as X-Ray diffraction (XRD), particle size analysis (PSA), scanning electron microscopy (SEM) and Blains specific surface area. The details of various tests performed on developed GEOPAV blocks are explained in following sections.

2.5.1. Dimension requirements and plan area

Vernier calliper was used to measure the length and width of the specimens across two opposite faces as per IS 15658–2021(Annex B). Two spots were chosen for length measurement and three spots for width measurement. The mean length and width of the GEOPAV blocks was recorded to the nearest 1 mm. Plan area (Asp) of paver block is required to determine the compressive strength of pavers. In this study, the pavers subjected to the compressive force was used for the plan area determination as per IS 15658–2021 (Annex B). For determining the plan area, the tested specimens were placed on the cardboard and its perimeter was traced and cut-out. The cut-out

Fig. 1. Precursor materials (a) SPFA and (b) BKRHA.

Table 1
Mix specifications evaluated.

GEOPAV mix type	NaOH molarity	SPFA (%)	BKRHA (%)
12GFA100	12	100	0
12GFR9505	12	95	5
10GFA100	10	100	0
10GFR9505	10	95	5

Table 2
Details of mix proportion.

Mix Ingredients	Mix type				
	CCP100	12GFA100	12GFR9505	10GFA100	10GFR9505
SPFA, kg/m^3	–	448	426	448	426
BKRHA, kg/m^3	–	0	22	0	22
Cement, kg/m^3	400	0	0	0	0
Na_2SiO_3, kg/m^3	–	180	180	180	180
NaOH, kg/m^3	–	70	70	70	70
Water, kg/m^3	220	0	0	0	0
CA, kg/m^3	1160	1104	1104	1104	1104
CSA, kg/m^3	570	598	598	598	598

samples were weighed using a weight balance of 0.0001 N accuracy and the results were noted as mass of testing sample (Msp). The same process was repeated with the cut-out rectangular cardboard of size 200 mm × 100 mm and was recorded as standard mass (Mstd). Using Eq. 1 the plan area was recorded in square millimetres.

$$Asp = 20000 \times \frac{Msp}{Mstd} \tag{1}$$

Where, 'Asp' is the plan area, 'Msp' is the mass of testing specimen area and 'Mstd' is the standard area. Table 3 presents the average plan area of all the design mixes, which is then used to calculate the compressive strength of GEOPAV blocks.

2.5.2. Compressive strength

The compressive strength of GEOPAV blocks was determined as per IS 15658–2021 (Annex D) specification. Compression testing machine with a digital supply and a pressure gauge having maximum capacity of 2000 kN was used. After recording the dimensions and plan area, the specimen is eccentrically placed between the bearing plates by adjusting the wearing surface in upward direction. Load was applied without shock and increased at a rate of 18 N/mm^2/ min till failure occurred in the block. The obtained load was noted and divided by the calculated plan area to get the destructive compressive strength. Fig. 2 shows the compressive strength test setup and failure of paver block.

2.5.3. Splitting tensile strength

Splitting tensile strength test of GEOPAV blocks was conducted in accordance with IS 15658–2021 using a compression testing machine of 500 kN capacity. The paver blocks were eccentrically situated between 75 mm rigid barrier and rubber strips of 15 mm wide and 3 mm thick. The test was performed by applying load parallel to the edges along the length of the splitting section of the block at a rate of 0.06 MPa/s, and a clear splitting failure was observed as shown in Fig. 3. The split tensile strength was calculated using Eq. 2.

$$T = 0.637 \times \frac{kP}{s} \tag{2}$$

Where, k = correction factor (i.e., 1), P is the failure load in 'N', and s is the failure plain area in mm^2.

Table 3
Plan area of conventional and GEOPAV blocks.

Mix type	Avg. M_{sp} (N)	Avg. M_{std} (N)	A_{sp} (mm^2)
CCP100	28.3402	18.9901	29847
12GFA100	29.0284	19.3408	30017
12GFR9505	29.0186	19.2074	30216
10GFA100	29.0622	19.3126	30096
10GFR9505	29.0681	19.2010	30278

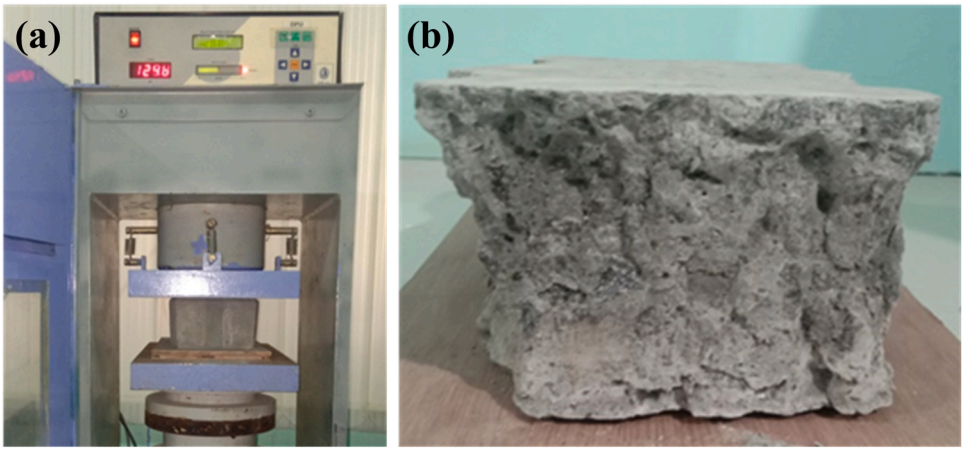

Fig. 2. (a) compressive strength test setup and (b) failure pattern.

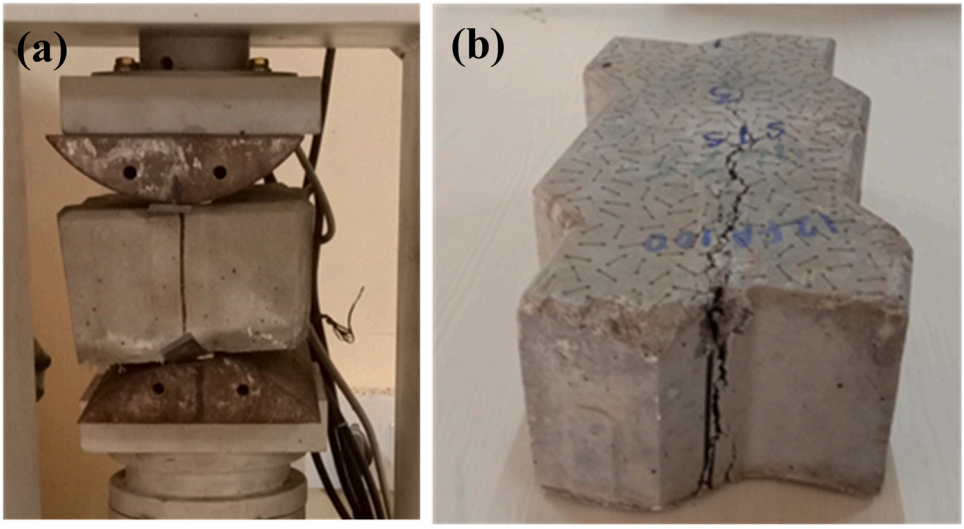

Fig. 3. (a) splitting tensile strength test setup and (b) failure pattern.

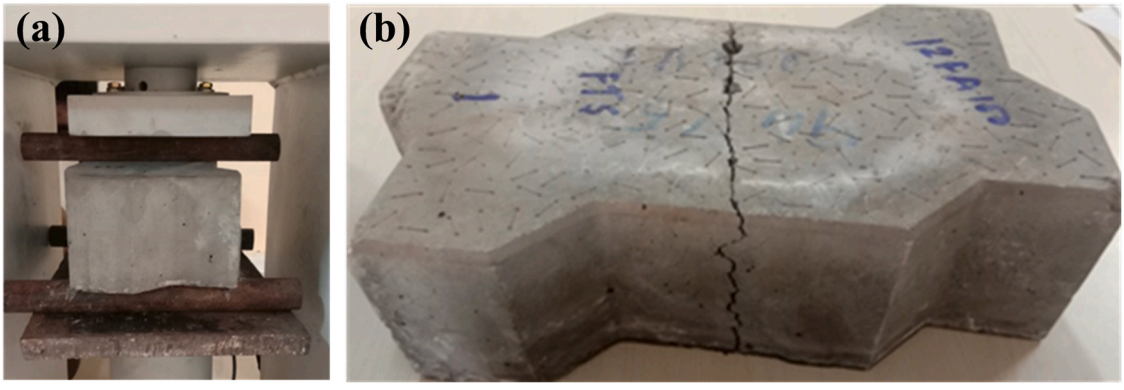

Fig. 4. (a) flexural strength test setup and (b) failure pattern.

2.5.4. Flexural strength

Flexural strength of GEOPAV blocks after 28 days curing was determined by three-point loading in accordance with IS 15658–2021 (Annex G) using a compression testing machine of 500 kN capacity. The paver blocks were placed between rollers of 25 mm, positioned halfway between supporting rollers in a loading pattern of simple beam as shown in Fig. 4. After positioning the specimen, the load was applied at a rate of 6.6 kN/min until the specimen fail in flexure. The resulting load at failure was recorded and used to determine the flexural strength using Eq. 3.

$$Fs = 1.5 \quad \times \quad \frac{fl}{bt^2} \tag{3}$$

Where, f is load at failure in 'N', l is the distance between the supporting rollers (i.e., 200 mm), b & t are the average width and thickness measured at fracture line.

2.5.5. Resistance to abrasion

This test was conducted in accordance with the procedure specified in IS 15658–2021. The 28 days ambient cured specimens of size 70 mm × 70 mm x 50 mm were cut and placed on the abrasion testing machine. The uniform load of 297 N was applied through the pressure stamp from the horizontal top surface and 22 rev/min were made as per specifications. High refractive index aluminium powder with approximately 95% aluminium oxide having moh's scale hardness of 9.0 and specific gravity of 3.95 was used as abrasion powder. The abrasion resistance of both control and GEOPAV samples were determined by measuring initial and final thickness using Vernier calliper. The impacts were compared to the maximum allowed limits of 2–2.5 mm for heavy movement and 3.5–4.0 mm for domestic wear applications as per IS 1237. Loss in volume in mm^3 per 5000 mm^2 was interpreted as per the IS 15658–2021 (Annex E).

2.5.6. Resistance to frost attack

This test was carried out in accordance with the ASTM C67 and IS 15658–2021 (Annex H) specifications. The specimen of approximate size 70 mm^3 was cut from the pavers and it was submerged in a cryostatic water bath. Fig. 5 shows the cryostatic water bath used in this study. The unit was subjected to 30 freezing and thawing cycles with each cycle comprising 16 h of freezing at − 9 °C and followed by 8 h of thawing at room temperature (27 ± 2 °C). The strength loss after 30 cycles was determined after washing the tested specimen in 3% sodium chloride (NaCl) solution.

2.5.7. Resistance to acid attack

The resistance to acid for GEOPAV blocks were studied after 28 days of ambient curing. The controlled and GEOPAV specimens were immersed in 5% laboratory grade sulphuric acid (H_2SO_4 purity of 98%) by covering with polyurethane cap upto 28 days. The pH of 2 for sulphuric acid was maintained throughout the experiment and it was monitored using a digital pH meter. After the acid immersion period, the specimens were taken out and dried in a room temperature (27 ± 2 °C, 65% humidity) for 72 h, followed by determination of strength loss of the respective specimens.

Fig. 5. Cryostatic water bath.

3. Results and discussion

3.1. Properties of raw materials

The GEOPAV blocks is composed of precursors and 12.5 mm down gravel materials. SPFA serves as the principal precursor and BKRHA as a supplementary secondary precursor. Generally, the morphology of SPFA is spherical particles that are primarily composed of silica. The primary precursor was evaluated as per ASTM C618 and IS 3812 (Part 1) specifications, and it confirms that the procured SPFA is of Class F category with spherical particles as shown in Fig. 6(a). BKRHA normally has high silica content (i.e., upto 90%), is light in weight and highly porous with a large exterior irregular surface area. Micro porous surface and honeycombed structures were observed in morphology as shown in Fig. 6(b), explaining the high surface area which will contribute to enhanced retention of water. BKRHA is affected by silica content, silica crystallisation stage, particle size and the surface region of fiery residue particles. For this study, the BKRHA obtained from N S brick industry of Ramnagaram city confirmed 88.84% silica content. Further, XRD pattern of SPFA clearly shows the presence of quartz, mullite and hematite as shown in Fig. 7. While XRD pattern of BKRHA contains the main constituent of SiO_2 in cristobalite and tridymite form which are referred as a mineral polymorph of silica that are formed at high temperature with a crystal system as tetragonal and hence the morphology of BKRHA is irregular. Also, a peak with broad full width at half maximum (i.e., ranging from 15° to 35°) confirms the amorphous nature of BKRHA. The chemical composition of SPFA and BKRHA is presented in Table 4. As seen, both SPFA and BKRHA is rich in silica which shall contribute towards geopolymerization in GEOPAV composites. The physical properties of SPFA and BKRHA are presented in Table 5. The fineness (percentage retained on 45 μm) for SPFA and BKRHA was 1.31% and 30% respectively, indicating that SPFA is finer than BKRHA. Further, specific gravity of SPFA and BKRHA was 2.08 and 1.97 respectively, which is similar to values reported in the previous studies [40,41]. The particle size distributions of aggregates are shown in Fig. 8. The fineness modulus of crushed stone dust (CSD) was 2.75, and according to IS 383 specification, CSD was categorized in grading zone II, indicating that selected CSD was not very fine. The physical properties of aggregates are presented in Table 6.

3.2. Fresh and hardened properties of GEOPAV blocks

3.2.1. Workability and unit weight

After preparation of fresh GEOPAV mix, the slump test was performed according to IS 1199. Fig. 9 shows the slump and unit weight of fresh mix. As seen, the addition of BKRHA has decreased the slump and unit weight values for both the mixes with varying molar ratios. The maximum unit weight and slump was observed for 12GFA100 mix (i.e., 2430 kg/m^3 and 210 mm) and a decreasing trend was noticed with the addition of BKRHA in the mix. The lower specific gravity of BKRHA in contrast to SPFA results in a reduction of unit weight. A reduction in slump can be attributed to the presence of high porous surface in BKRHA combined with the viscous nature of alkali solution.

3.2.2. Visual inspection, dimensions and tolerances and plan area

A visual evaluation of the quality of the paving blocks was conducted in natural daylight. The blocks were set out on a level floor in a chosen paving pattern, covering area of one square meter. The visible faults in paving blocks such as cracks and flaking were recorded by inspecting the paving blocks from a distance of approximately one metre. The observation revealed that all GEOPAV blocks were free of cracks and defects and showed high quality in finish and appearance. The specifications of ASTM C 936 describes that the exposed area facing should be less than 0.065 m^2 and aspect ratio (ratio of overall length to thickness) should be less than 4. The dimensions and tolerances of the pavers influence the structural efficiency of paving blocks. The maximum difference of + 1 mm in

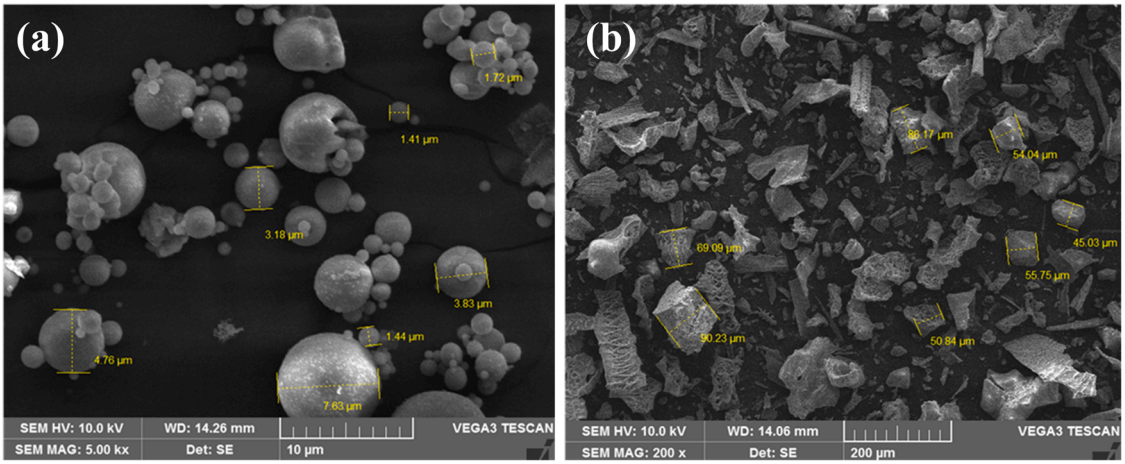

Fig. 6. SEM image of (a) SPFA and (b) BKRHA.

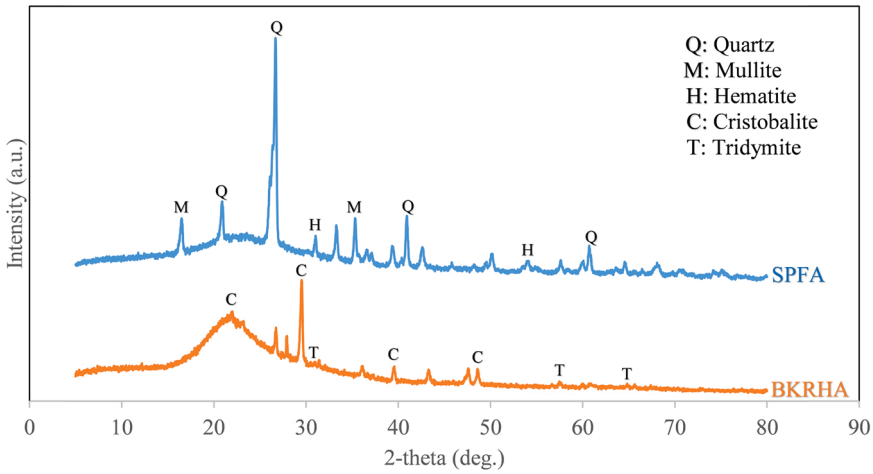

Fig. 7. XRD pattern of SPFA and BKRHA.

Table 4
Chemical composition of SPFA and BKRHA.

Constituents	SPFA %, by mass	BKRHA %, by mass
SiO_2	63.23	88.84
Al_2O_3	24.55	0.81
Fe_2O_3	5.18	0.83
CaO	2.80	2.38
MgO	1.32	0.44
SO_3	0.45	0.35
Na_2O	1.20	0.78
K_2O	0.19	2.06
Total chloride	0.008	0.007
Loss on Ignition	1.07	3.49

Table 5
Physical properties of SPFA and BKRHA.

Tested parameters	SPFA	BKRHA
Specific gravity	2.08	1.97
Surface area (cm^2/g)	488	340
Material retained on 45 μm sieve (%)	1.35	30
Particle shape	Spherical	Irregular
Average particle size (microns)		
D10 (μm)	< 6	< 4
D50 (μm)	< 5	< 6
D90 (μm)	< 14	< 20

length was observed for 10GFA100 and 10GFR9505. Similarly, the maximum difference of − 1 mm was observed in width for CCP100 mix and a maximum difference of + 1 mm in thickness was observed for 12GFR9505, 10GFR9505 and CCP100 mixes. The obtained results for all mix types was found to be within the tolerance limits. Table 7 presents the details of results for dimensions and tolerances along with the limitations for length, width, and thickness as per IS 15658–2021.

3.2.3. *Compressive strength*

Fig. 10 shows the average compressive strength of 12GFA100, 12GFR9505, 10GFA100 and 10GFR9505 specimens at the ages of 28 and 56 days. As seen, the addition of BKRHA has slightly increased the compressive strength for both the molar ratios. The strength increment can be attributed to the siliceous gel formation due to presence of BKRHA. However, this increment is not very significant with curing age, and similar findings were reported when 3% and 7% fly ash was replaced with microwave incinerated rice husk ash [38]. It is also seen that at moderate exposure conditions (i.e., 45 ºC) all the geopolymer mixes with and without BKRHA were able to achieve desirable compressive strength, suggesting an effective dissolution of aluminosilicate species for all the mix types. Further, in comparison to CCP100, the GEOPAV blocks showed much better performance in terms of compressive strength. For instance, the

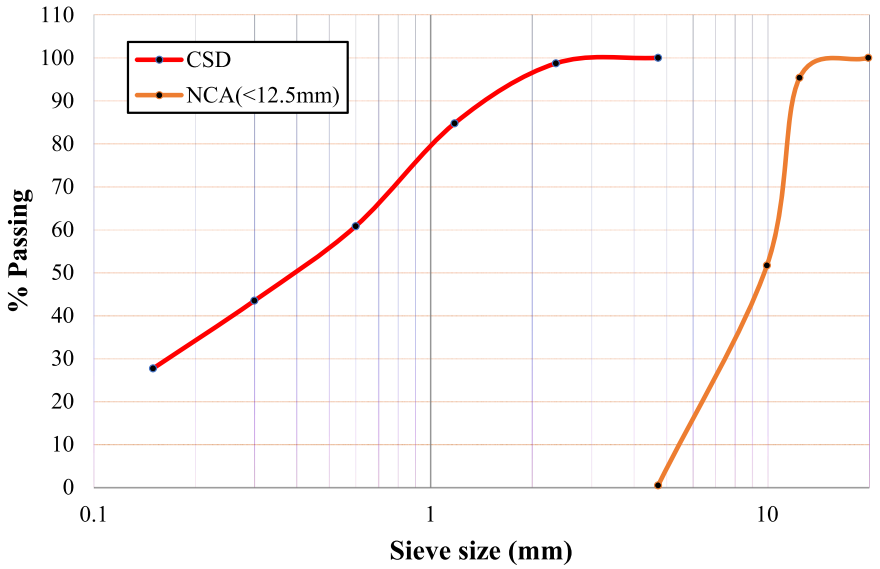

Fig. 8. Particle size distribution of aggregates.

Table 6
Physical properties of aggregates.

Tested parameters	CSD	NCA
Specific gravity	2.56	2.65
Water absorption (%)	1.95	0.92
Density (kg/m^3)		
Loose	1700	1400
Rodded	1900	1500
Particle passing 75 μm (%)	15	0.6

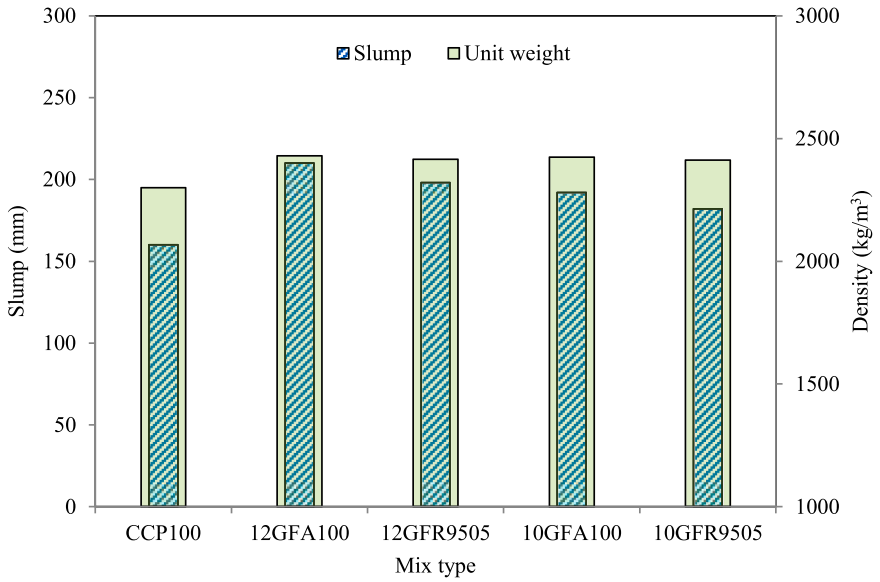

Fig. 9. Effect of BKRHA on fresh properties of GEOPAV blocks.

increase in compressive strength at 28 days was observed to be 30%, 31%, 26% and 29% for 12GFA100, 12GFR9505, 10GFA100 and 10GFR9505 mixes when compared to CCP100 mix, respectively. Similarly, the increase in compressive strength at 56 days was observed to be 21%, 22%, 17% and 20% for 12GFA100, 12GFR9505, 10GFA100 and 10GFR9505 mixes when compared to CCP100

Table 7
Dimensions and tolerances of conventional and GEOPAV blocks.

Mix type	Length (l, mm)	Width (w, mm)	Thickness (t, mm)	Aspect ratio(l/t)
CCP100	250	119	81	3.09
12GFA100	250	120	80	3.13
12GFR9505	250	120	81	3.09
10GFA100	251	120	80	3.14
10GFR9505	251	120	81	3.10

Note: Standard size: L = 250 mm, W = 120 mm, T = 80 mm & L/T = 3.125. Tolerances as per IS 15658–2021 for length and width = ± 2 mm, for thickness = ± 3 mm

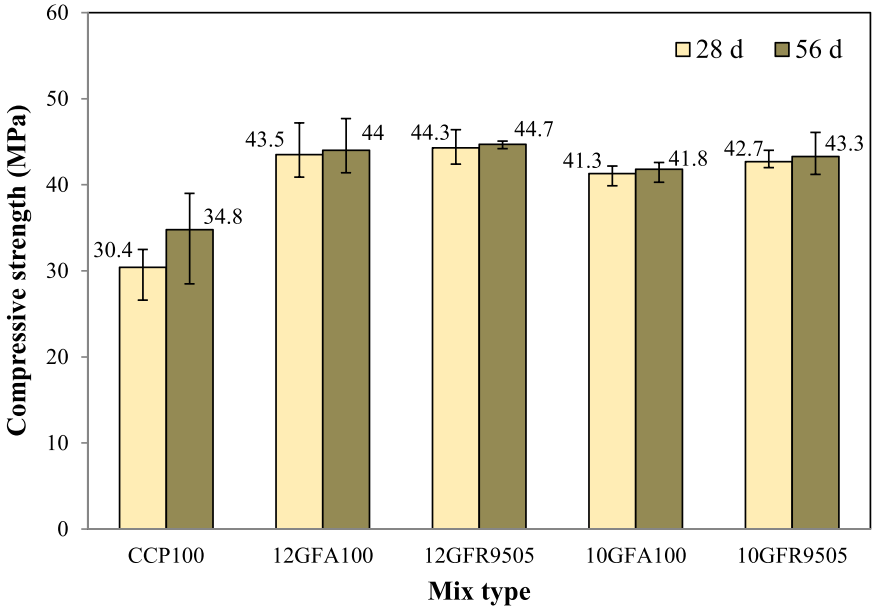

Fig. 10. Compressive strength of pavers at 28 and 56 days.

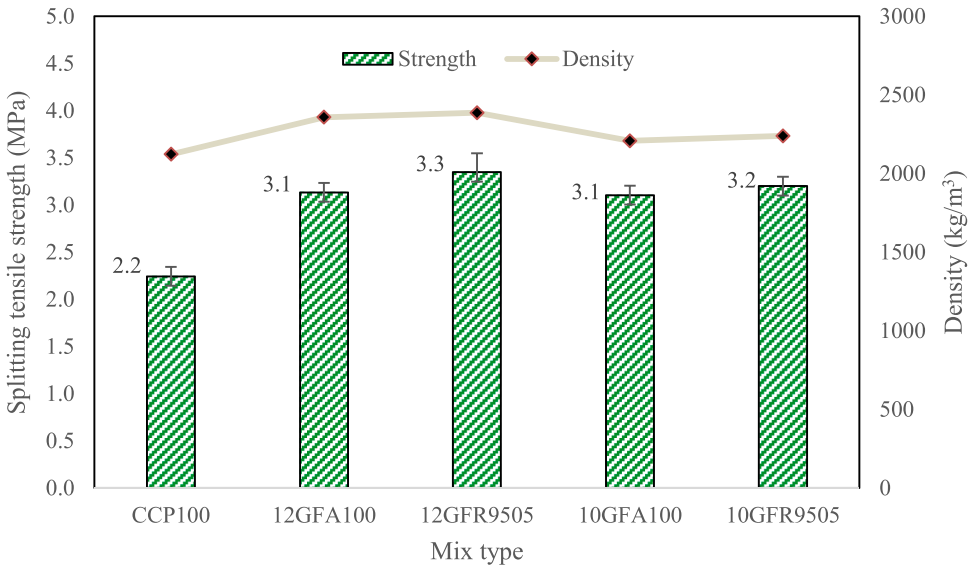

Fig. 11. Split tensile strength and density at 28 days curing.

mix. This clearly shows the potential for GEOPAV blocks to perform much better than conventional paver blocks in service. The Indian standard specifies that the compressive strength of the pavers should not be less than 30 MPa for non-traffic application and 40 MPa for medium-traffic applications. In particular, the pavers which have 80 mm thickness should perform under the medium traffic category, and all the GEOPAV blocks satisfy this standard requirement.

3.2.4. Splitting tensile strength

Fig. 11 shows the splitting tensile strength of the paving blocks at 28 days curing for both molar ratios. For GEOPAV blocks, split tensile strength increased with the addition of BKRHA. This improvement can be attributed to a better reaction and high silica content in BKRHA, which contributes to the formation of much stronger Si-O-Si bond, and also improves the microstructure, making it denser and compact [42]. This has also resulted in slight increase in density of GEOPAV blocks with BKRHA, when compared to plain GEOPAV blocks and CCP100. Further, GEOPAV blocks showed better split tensile strength when compared to conventional paver blocks. For instance, 12GFA100 and 12GFR9505 demonstrated 29% and 33% higher strength than control mix CCP100, respectively. Similarly, 10GFA100 and 10GFR9505 demonstrated 29% and 31% higher strength than control mix CCP100, respectively. According to IS 15658–2021, M40 grade pavers should achieve a minimum split tensile strength of 3 N/mm^2 after 28 days curing, and all the GEOPAV blocks satisfy this requirement.

3.2.5. Flexural strength

Fig. 12 shows the 28 days flexural strength for the paver blocks. As seen, the addition of BKRHA has significantly improved the flexural strength of GEOPAV blocks. An improved flexural strength for GEOPAV with BKRHA is directly beneficial for paver blocks to perform better in service, since resistance to fracture and failure due to uneven and sudden force is improved when flexural strength of paver blocks increases. The improvement in flexural strength of mixes with BKRHA can be attributed to increased SiO_2/Al_2O_3 ratio, which further enhances the microstructure of geopolymer paste and the interfacial transition zone that becomes stronger [42]. Also, the tensile properties of alkali-activated concrete with rice husk ash have shown to be better, due to stronger bond between the alkali-activated gel and the aggregates [43]. This has resulted the GEOPAV blocks with BKRHA to perform better among all the mixes. Further, the GEOPAV blocks have also shown significantly higher flexural strength when compared to control mix CCP100. For instance, there was 42% and 46% increase in flexural strength for 12GFA100 and 12GFR9505 when compared to CCP100, respectively. Similarly, there was 36% and 41% increase in flexural strength for 10GFA100 and 10GFR9505 when compared to CCP100, respectively. It is also observed that the effect of NaOH molarity on strength properties of GEOPAV with BKRHA was not significant. According to IS 15658–2021 specification the average flexural strength for paver blocks should achieve a minimum of $0.11f_{ck}$. For this study, the compressive strength 'f_{ck}' was approximately 40 N/mm^2. Therefore, the minimum specified flexural strength as per the standard would be 4.4 MPa, and all the GEOPAV mixes satisfy this requirement.

3.3. Durability properties of GEOPAV blocks

3.3.1. Water absorption

Water absorption is crucial to determine the porous nature of the paver blocks. This test was conducted after 28 days of curing and effect of BKRHA on water absorption of GEOPAV blocks is shown in Fig. 13. According to IS 15658–2021 (Annex C) the water absorption is limited to an average of 6% by mass. The results show that all GEOPAV mixes satisfy the requirements of codal provision. It was also observed that there was an increase in water absorption for GEOPAV blocks with BKRHA. The increase in water absorption in BKRHA mixes can be attributed to the presence of high porous nature of the binder. Further, when the paver blocks are heated in oven at 110ºC, it evaporates the water occupied by pores of BKRHA and results in the increase of GEOPAV block absorption. Also, all GEOPAV blocks show lower water absorption when compared to control mix CCP100. For instance, the water absorption at 28 days was reduced by 34%, 24%, 7% and 3.4% for 12GFA100, 12GFR9505, 10GFA100 and 10GFR9505 when compared to CCP100 mix, respectively. Such findings ascertain the improved microstructure of the GEOPAV mixes in contrast to the conventional concrete mixtures CCP100.

3.3.2. Resistance to abrasion

The resistance to wear is crucial when the surface of paver blocks is exposed to traffic movements. The addition of BKRHA has resulted in decrease in volume loss as shown in Fig. 14. For instance, at 28 days, the decrease in volume and thickness loss was 16% and 14% for 12GFR9505 when compared to 12GFA100, respectively. Similarly, at 28 days, the decrease in volume and thickness loss was 8.3% and 9.4% for 10GFR9505 when compared to 10GFA100, respectively. Such improvements for BKRHA incorporated GEOPAV blocks can be attributed to densification of the microstructure and improved bonding with the aggregate particles, which enhances the resistance to abrasion. Also, addition of rice husk ash in alkali-activated concrete develops a stronger interfacial bond due to fine RHA particles acting as micro-filler, which improves bond between aggregate and the gel, and thus improves abrasion resistance [43]. Further, all the GEOPAV blocks performed better in resisting the abrasive force when compared to control mix CCP100. Thus, indicating much better performance for GEOPAV blocks in service, when compared to existing commercial paver blocks.

3.3.3. Resistance to frost and acid attack

Resistance to freezing and thawing is an essential metric in evaluating the durability properties of concrete, particularly in places where temperature is extremely low. Frost resistance is measured by the proportion of strength loss due to freeze-thaw cycles. The frost resistance study is relatively well established for OPC concrete and limited for geopolymer concrete. Fig. 15 shows the results of frost

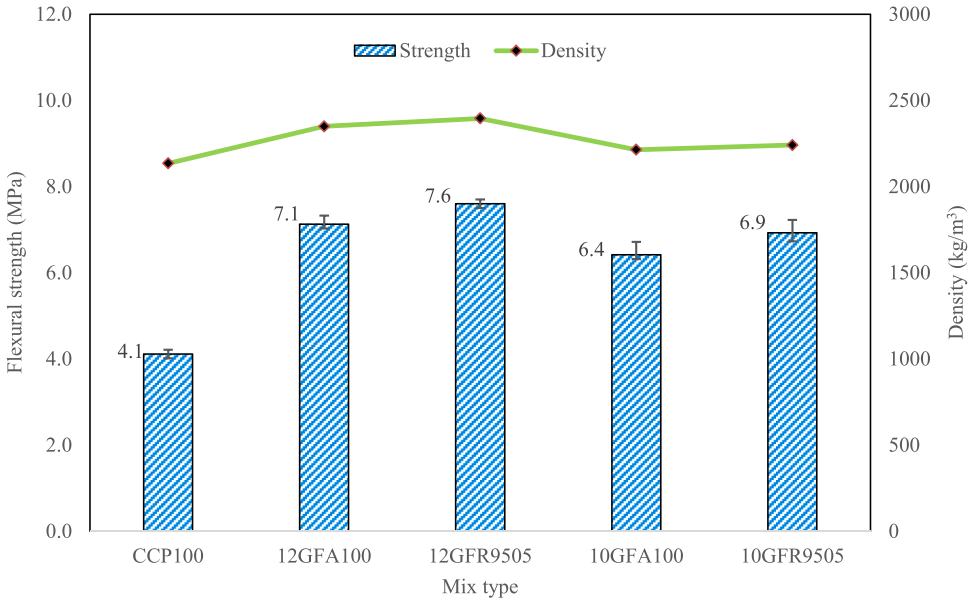

Fig. 12. Flexural strength and density at 28 days of curing.

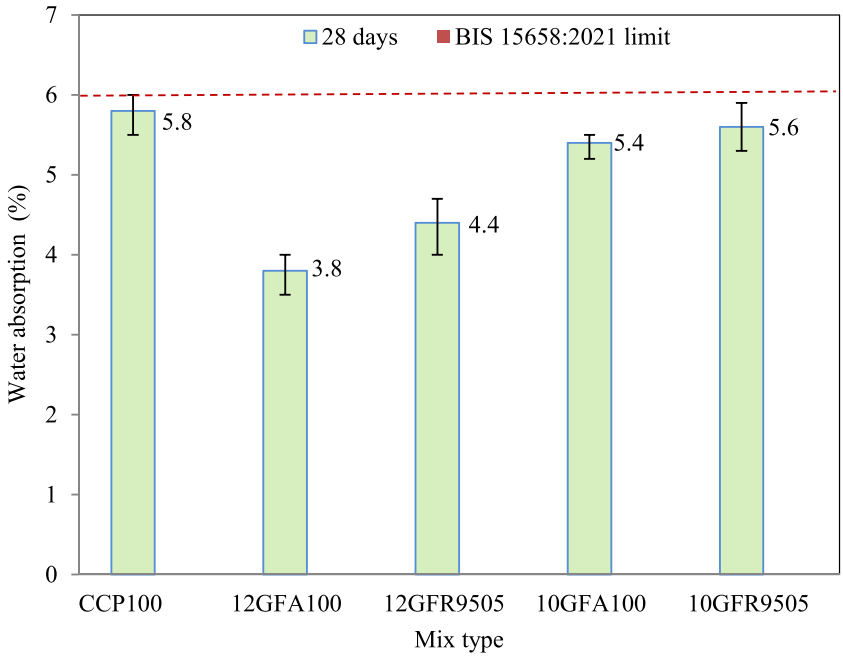

Fig. 13. Effect of BKRHA on water absorption of GEOPAV blocks.

and acid attack on the GEOPAV blocks. As seen, the addition of BKRHA has improved the resistance towards acid and frost attack for GEOPAV blocks. For instance, irrespective of the molar ratios, addition of BKRHA has reduced the strength loss due to acid and frost attack. Such improvements in durability properties can be attributed to higher silica species present in BKRHA. Also, dissolution of silica species from BKRHA particles significantly contribute towards improvement in Si/Al ratio trend of SPFA-BKRHA based specimen [38]. Further, formation of Si-O-Si based geopolymer results in enhancement of microstructure, making it denser and thus contributing towards better resistance to acid and frost attack for SPFA-BKRHA specimens. Furthermore, one of the primary reasons for improvement in durability of alkali-activated concrete with RHA is due to extensive refinement of the pore structure, and the fine RHA particles have tendency to fill the voids, which also enhances the density of the blocks and improves the durability properties [43].

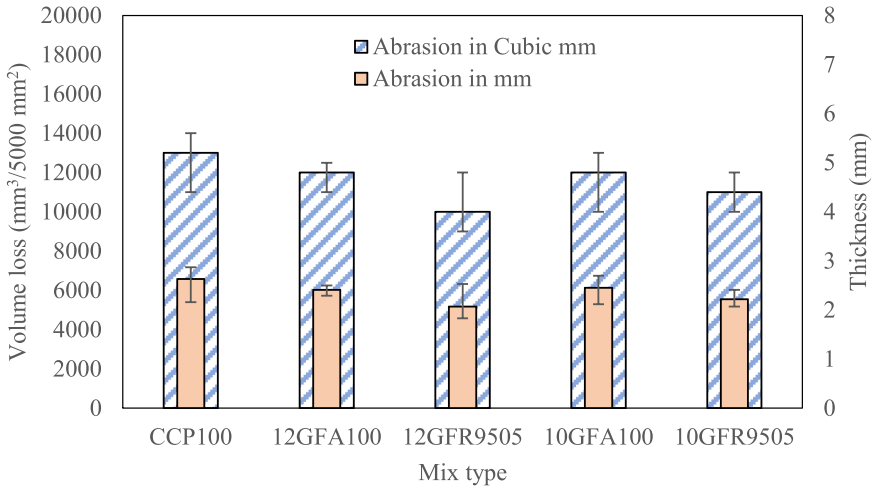

Fig. 14. Effect of BKRHA on abrasion resistance of GEOPAV blocks.

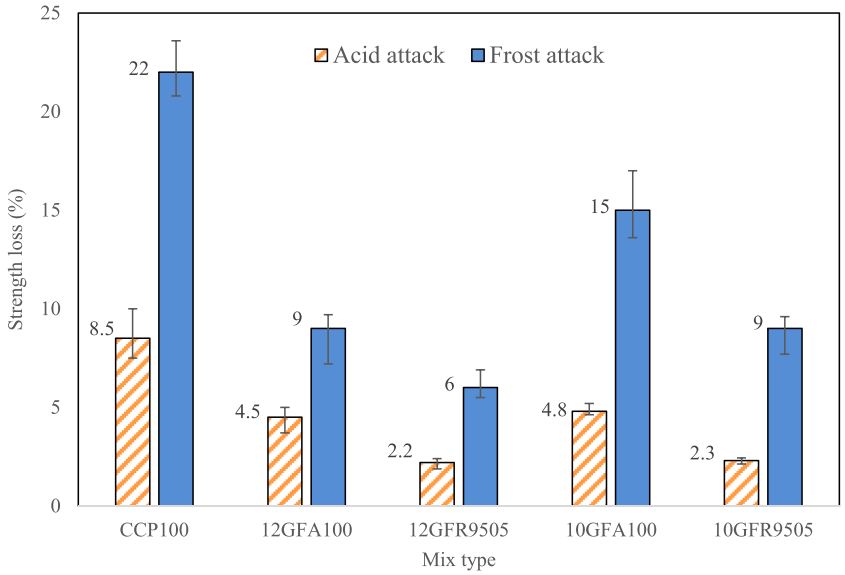

Fig. 15. Strength loss for GEOPAV blocks due to acid and frost attack.

3.4. Microstructural analysis of GEOPAV blocks

Fig. 16 shows the microstructure of GEOPAV blocks. The mixes 10GFA100 and 12GFA100 appear with slightly larger voids and openness in gel formation, which is probably caused during crystallization of gel phase and hydration function. The micro cracks began to reduce along with the refinement of voids leading to densified gel formations in samples of 10GFR9505 and 12GFR9505, attributing to the presence of BKRHA in the matrix. These findings persuasively testify that the addition of BKRHA is beneficial in the formation of a dense microstructure and homogeneity in geopolymer matrix due to the presence of high amounts of reactive silica in BKRHA. The results from energy-dispersive X-Ray spectroscopy (EDAX) were also interpreted. Accordingly, the reactive gel compounds in GEOPAV blocks were the oxides of silica and alumina. The 10GFA100, 10GFR9505, 12GFA100 and 12GFR9505 had silica to alumina ratio (SiO_2/ Al_2O_3) of 2.7, 3.3, 2.5 and 2.6, respectively. Similarly, the calcium oxide content was 1.17, 2.5, 0.77 and 0.85, respectively. The observations indicate that the dense formation of GEOPAV was due to the addition of BKRHA which increase the Si-O-Al bond during hardening process.

Fig. 17 shows the XRD images of hardened GEOPAV composites. According to the obtained results, quartz and anorthite are the main crystallized products in hardened GEOPAV blocks. The peak intensity of anorthite phase enhanced with addition of BKRHA, which is assigned to the silicon source from BKRHA promoting the more formation of Na-Al-Si_3-O_8 gel. Further, most XRD images for GEOPAV blocks exhibited a major crystalline peak of quartz. However, the main difference was observed with the addition of BKRHA,

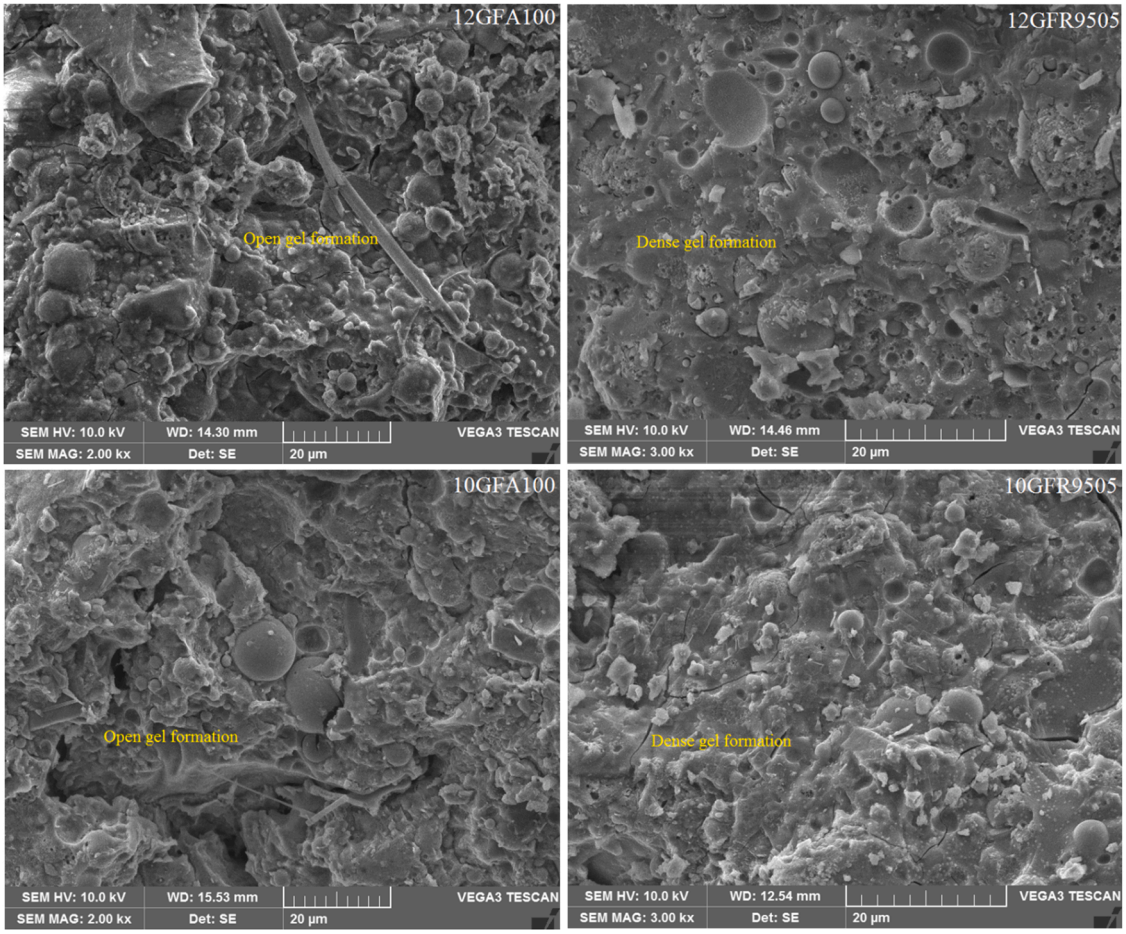

Fig. 16. SEM images of GEOPAV blocks.

that there is a decrease in the intensity of this crystalline peaks. This behaviour can be attributed to partial dissolution of the silicate minerals in BKRHA and thereby contributing towards formation of polymeric gel, which serve as a binder in further enhancing the microstructure of the geopolymer matrix. Thus, it was observed from the durability studies that all GEOPAV blocks with BKRHA performed better in terms of resistance to acid and frost attack, suggesting the positive influence of BKRHA in GEOPAV blocks.

4. Conclusions

In present study GEOPAV blocks are developed with blend of SPFA, BKRHA, natural aggregates and alkaline activators, and cured in both sundry and room temperature conditions. Fresh, mechanical and durability properties of GEOPAV blocks are evaluated and compared with conventional paver blocks. Based on experimental study following important findings and conclusion is enumerated.

1. Replacement of SPFA with BKRHA has reduced the workability of GEOPAV mixes. This can be attributed to microporous and honeycombed structure in the morphology of BKRHA particles.
2. When SPFA was replaced with 5% BKRHA, there was negligible improvement in compressive strength of GEOPAV blocks. However, for same mixes significant improvement in split tensile strength and flexural strength was observed, along with improved density for hardened GEOPAV blocks. Such findings indicate refinement of microstructure due to addition of BKRHA. Further, the strength properties of GEOPAV blocks were far superior than conventional paver blocks.
3. GEOPAV blocks showed improved resistance to abrasion when compared to conventional paver blocks and this was further enhanced with addition of 5% BKRHA, indicating a good bond between alkali-activated gel and the aggregates.
4. The incorporation of BKRHA in GEOPAV blocks has significantly improved the resistance to acid attack and frost attack. The improved durability properties for BKRHA-GEOPAV blocks can be attributed to dense polymeric gel formations, which is primarily due to high content of amorphous silica in BKRHA.

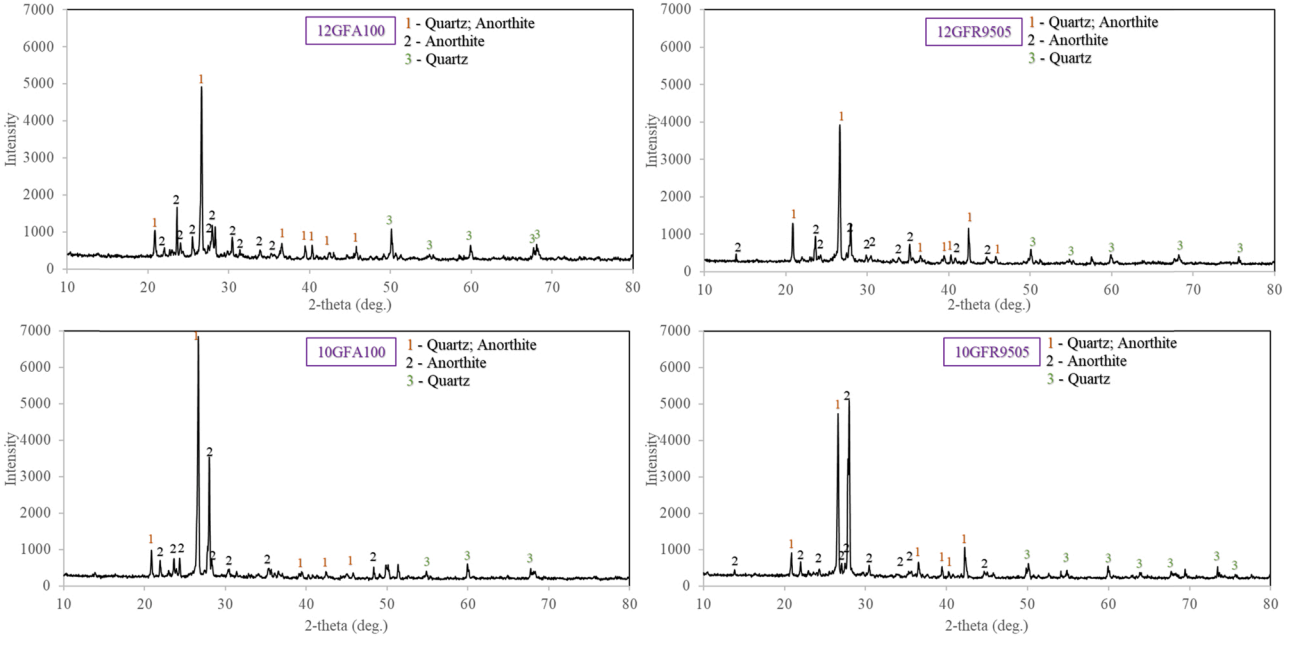

Fig. 17. XRD of GEOPAV composites.

5. Based on the results of this study all the GEOPAV blocks satisfy the requirement of IS 15658–2021 and can be used for various paving applications. Further, the performance of GEOPAV blocks improved when SPFA was replaced with 5% BKRHA and this will influence the quality and service life of paver blocks.

Declaration of Competing Interest

The authors declare that they have no known competing financial interests or personal relationships that could have appeared to influence the work reported in this paper.

Acknowledgment

The authors gratefully acknowledge centre for research in social science and education at JAIN (Deemed to be University). Appreciation is also extended to ISO labs, Bangalore, for providing facilities during this study.

References

[1] Ministry of Urban Development, Preparing a comprehensive mobility plan (CMP) - A toolkit (revised 2014), Government of India, 2014.
[2] A.R.G. de Azevedo, C.M.F. Vieira, W.M. Ferreira, K.C.P. Faria, L.G. Pedroti, B.C. Mendes, Potential use of ceramic waste as precursor in the geopolymerization reaction for the production of ceramic roof tiles, J. Build. Eng. 29 (2020), https://doi.org/10.1016/j.jobe.2019.101156.
[3] A.R.G. de Azevedo, M.T. Marvila, H.A. Rocha, L.R. Cruz, C.M.F. Vieira, Use of glass polishing waste in the development of ecological ceramic roof tiles by the geopolymerization process, Int. J. Appl. Ceram. Technol. 17 (6) (2020) 2649–2658, https://doi.org/10.1111/ijac.13585.
[4] A.R.G. de Azevedo, M.T. Marvila, M. Ali, M.I. Khan, F. Masood, C.M.F. Vieira, Effect of the addition and processing of glass polishing waste on the durability of geopolymeric mortars, Case Stud. Constr. Mater. 15 (2021), https://doi.org/10.1016/j.cscm.2021.e00662.
[5] M. Amran, A. Al-Fakih, S.H. Chu, R. Fediuk, S. Haruna, A. Azevedo, N. Vatin, Long-term durability properties of geopolymer concrete: an in-depth review, Case Stud. Constr. Mater. 15 (2021), https://doi.org/10.1016/j.cscm.2021.e00661.
[6] F.H.A. Zaidi, R. Ahmed, M.M.A.B. Abdullah, S.Z.A. Rahim, Z. Yahya, L.Y. Li, R. Ediati, Geopolymer as underwater concreting material: A review, Constr. Build. Mater. 291 (2021), https://doi.org/10.1016/j.conbuildmat.2021.123276.
[7] E.A. Azimi, M.M.A.B. Abdullah, P. Vizureanu, M.A.A.M. Salleh, A.V. Sandu, J. Chaiprapa, S. Yoriya, K. Hussin, I.K. Aziz, Strength development and elemental distribution of dolomite/fly ash geopolymer composite under elevated temperature, Materials 13 (4) (2020) 1015, https://doi.org/10.3390/ma13041015.
[8] M. Pyngrope, N. Hossiney, Y. Chen, H.K. Thejas, C.K. Sarath, J. Alex, S.L. Kumar, Properties of alkali-activated concrete (AAC) incorporating demolished building waste (DBW) as aggregates, Cogent Eng. 8 (1) (2021), https://doi.org/10.1080/23311916.2020.1870791.
[9] M. Yusuf, Agro-industrial waste materials and their recycled value-added applications: review. In Handbook of Ecomaterials, Springer Science and Business Media LLC, Berlin, Germany, 2017, pp. 1–11.
[10] E. Cintura, L. Nunes, B. Esteves, P. Faria, Agro-industrial wastes as building insulation materials: a review and challenges for Euro-Mediterranean countries, Ind. Crops Prod. 171 (2021), https://doi.org/10.1016/j.indcrop.2021.113833.
[11] M.V. Madurwar, R.V. Ralegaonkar, S.A. Mandavgane, Application of agro-waste for sustainable construction materials: A review, Constr. Build. Mater. 38 (2013) 872–878, https://doi.org/10.1016/j.conbuildmat.2012.09.011.
[12] FAO, World Food and Agriculture – Statistical Pocketbook 2020, Food and Agriculture Organization of the United Nations (FAO), Rome, 2020.
[13] J. Prasara, S.H. Gheewala, Sustainable utilization of rice husk ash from power plants: a review, J. Clean. Prod. 167 (2017) 1020–1028, https://doi.org/10.1016/j.jclepro.2016.11.042.
[14] D. Liu, W. Zhang, H. Lin, Y. Li, H. Lu, Y. Wang, A green technology for the preparation of high capacitance rice husk-based activated carbon, J. Clean. Prod. 112 (2016) 1190–1198, https://doi.org/10.1016/j.jclepro.2015.07.005.
[15] G.H.M.J.S. De Silva, B.V.A. Perera, Effect of waste rice husk ash (RHA) on structural, thermal and acoustic properties of fired clay bricks, J. Build. Eng. 18 (2018) 252–259, https://doi.org/10.1016/j.jobe.2018.03.019.
[16] S. Maithel, D. Lalchandani, G. Malhotra, P. Bhanware, Greentech Knowledge Solutions Pvt. Ltd., New Delhi (India), 2012.
[17] M.R. Karim, M.F.M. Zain, M. Jamil, F.C. Lai, Fabrication of a non-cement binder using slag, palm oil fuel ash and rice husk ash with sodium hydroxide, Constr. Build. Mater. 49 (2013) 894–902, https://doi.org/10.1016/j.conbuildmat.2013.08.077.
[18] R.S. Bie, X.F. Song, Q.Q. Liu, X.-Y. Ji, P. Chen, Studies on effects of burning conditions and rice husk ash (RHA) blending amount on the mechanical behavior of cement, Cem. Concr. Compos. 55 (2015) 162–168, https://doi.org/10.1016/j.cemconcomp.2014.09.008.
[19] V. Jittin, A. Bahurudeen, S.D. Ajinkya, Utilisation of rice husk ash for cleaner production of different construction products, J. Clean. Prod. 263 (2020), https://doi.org/10.1016/j.jclepro.2020.121578.
[20] B. Chatveera, P. Lertwattanaruk, Durability of conventional concretes containing black rice husk ash, J. Environ. Manag. 92 (1) (2011) 59–66, https://doi.org/10.1016/j.jenvman.2010.08.007.
[21] B. Chatveera, P. Lertwattanaruk, Evaluation of nitric and acetic acid resistance of cement mortars containing high-volume black rice husk ash, J. Environ. Manag. 133 (2014) 365–373, https://doi.org/10.1016/j.jenvman.2013.12.010.
[22] W. Chalee, T. Sasakul, P. Suwanmaneechot, C. Jaturapitakkul, Utilization of rice husk–bark ash to improve the corrosion resistance of concrete under 5-year exposure in a marine environment, Cem. Concr. Compos. 37 (2013) 47–53, https://doi.org/10.1016/j.cemconcomp.2012.12.007.
[23] G.S. Iam, N. Makul, Self-compacting concrete prepared using rice husk ash waste from electric power plants, Adv. Mater. Res. 488–489 (2012) 258–262, https://doi.org/10.4028/www.scientific.net/AMR.488-489.258.
[24] J. Alex, J. Dhanalakshmi, B. Ambedkar, Experimental investigation on rice husk ash as cement replacement on concrete production, Constr. Build. Mater. 127 (2016) 353–362, https://doi.org/10.1016/j.conbuildmat.2016.09.150.
[25] V. Kannan, K. Ganesan, Chloride and chemical resistance of self-compacting concrete containing rice husk ash and metakaolin, Constr. Build. Mater. 51 (2014) 225–234, https://doi.org/10.1016/j.conbuildmat.2013.10.050.
[26] M. Safiuddin, J.S. West, K.A. Soudki, Properties of freshly mixed self-consolidating concretes incorporating rice husk ash as a supplementary cementing material, Constr. Build. Mater. 30 (2012) 833–842, https://doi.org/10.1016/j.conbuildmat.2011.12.066.
[27] R.K. Sandhu, R. Siddique, Influence of rice husk ash (RHA) on the properties of self-compacting concrete: a review, Constr. Build. Mater. 153 (2017) 751–764, https://doi.org/10.1016/j.conbuildmat.2017.07.165.
[28] A. Mehta, R. Siddique, Sustainable geopolymer concrete using ground granulated blast furnace slag and rice husk ash: Strength and permeability properties, J. Clean. Prod. 205 (2018) 49–57, https://doi.org/10.1016/j.jclepro.2018.08.313.
[29] S. Yaseri, V.M. Verki, M. Mahdikhani, Utilization of high volume cement kiln dust and rice husk ash in the production of sustainable geopolymer, J. Clean. Prod. 230 (2019) 592–602, https://doi.org/10.1016/j.jclepro.2019.05.056.
[30] S. Mayooran, S. Ragavan, N. Sathiparan, Comparative study on open air burnt low- and high-carbon rice husk ash as partial cement replacement in cement block production, J. Build. Eng. 13 (2017) 137–145, https://doi.org/10.1016/j.jobe.2017.07.011.
[31] G.H.M.J.S. De Silva, M.L.C. Surangi, Effect of waste rice husk ash on structural, thermal and run-off properties of clay roof tiles, Constr. Build. Mater. 154 (2017) 251–257, https://doi.org/10.1016/j.conbuildmat.2017.07.169.

[32] H. Moayedi, B. Aghel, M.M. Abdullahi, H. Nguyen, A.S.A. Rashid, Applications of rice husk ash as green and sustainable biomass, J. Clean. Prod. 237 (2019), https://doi.org/10.1016/j.jclepro.2019.117851.
[33] K. Jankovic, D. Nikolic, D. Bojovic, Concrete paving blocks and flags made with crushed brick as aggregate, Constr. Build. Mater. 28 (1) (2012) 659–663, https://doi.org/10.1016/j.conbuildmat.2011.10.036.
[34] N. Hossiney, H.K. Sepuri, M.K. Mohan, A.H.R.S. Govindaraju, J. Chyne, Alkali-activated concrete paver blocks made with recycled asphalt pavement (RAP) aggregates, Case Stud. Constr. Mater. 12 (2020), https://doi.org/10.1016/j.cscm.2019.e00322.
[35] N. Hossiney, H.K. Sepuri, M.K. Mohan, S. Chandra, K.S.L. Kumar, T. H K, Geopolymer concrete paving blocks made with Recycled Asphalt Pavement (RAP) aggregates towards sustainable urban mobility development, Cogent Eng. 7 (1) (2020), https://doi.org/10.1080/23311916.2020.1824572.
[36] Y. Liu, Y. Zhuge, Christopher W.K. Chow, Alexandra Keegan, Danda Li, Phuong Ngoc Pham, Jianyin Huang, Rafat Siddique, Utilization of drinking water treatment sludge in concrete paving blocks: microstructural analysis, durability and leaching properties, J. Environ. Manag. 262 (2020), https://doi.org/10.1016/j.jenvman.2020.110352.
[37] E. Ganjian, G. Jalull, H. Sadeghi Pouya, Using waste materials and by-products to produce concrete paving blocks, Constr. Build. Mater. 77 (2015) 270–275, https://doi.org/10.1016/j.conbuildmat.2014.12.048.
[38] A. Kusbiantoro, M.F. Nuruddin, N. Shafiq, S.A. Qazi, The effect of microwave incinerated rice husk ash on the compressive and bond strength of fly ash based geopolymer concrete, Constr. Build. Mater. 36 (2012) 695–703, https://doi.org/10.1016/j.conbuildmat.2012.06.064.
[39] Y.J. Patel, N. Shah, Enhancement of the properties of ground granulated blast furnace slag based self compacting geopolymer concrete by incorporating rice husk ash, Constr. Build. Mater. 171 (2018) 654–662, https://doi.org/10.1016/j.conbuildmat.2018.03.166.
[40] M. Jamil, M.N.N. Khan, M.R. Karim, A.B.M.A. Kaish, M.F.M. Zain, Physical and chemical contributions of Rice Husk Ash on the properties of mortar, Constr. Build. Mater. 128 (2016) 185–198, https://doi.org/10.1016/j.conbuildmat.2016.10.029.
[41] S. Abbas, S.M.S. Kazmi, M.J. Munir, Potential of rice husk ash for mitigating the alkali-silica reaction in mortar bars incorporating reactive aggregates, Constr. Build. Mater. 132 (2017) 61–70, https://doi.org/10.1016/j.conbuildmat.2016.11.126.
[42] P. Nuaklong, P. Jongvivatsakul, T. Pothisiri, V. Sata, P. Chindaprasirt, Influence of rice husk ash on mechanical properties and fire resistance of recycled aggregate high-calcium fly ash geopolymer concrete, J. Clean. Prod. 252 (2020), https://doi.org/10.1016/j.jclepro.2019.119797.
[43] S. Fernando, M.C.M. Nasvi, C. Gunasekara, D.W. Law, S. Setunge, R. Dissanayake, Systematic review on alkali-activated binders blended with rice husk ash, J. Mater. Civ. Eng. 33 (9) (2021), https://doi.org/10.1061/(ASCE)MT.1943-5533.0003825.